

COMPARISON OF NONLINEAR RANDOM RESPONSE USING EQUIVALENT LINEARIZATION AND NUMERICAL SIMULATION

Stephen A. Rizzi[†] and Alexander A. Muravyov[‡]

NASA Langley Research Center
Structural Acoustics Branch
Hampton, VA 23681-2199

ABSTRACT

A recently developed finite-element-based equivalent linearization approach for the analysis of random vibrations of geometrically nonlinear multiple degree-of-freedom structures is validated. The validation is based on comparisons with results from a finite element based numerical simulation analysis using a numerical integration technique in physical coordinates. In particular, results for the case of a clamped-clamped beam are considered for an extensive load range to establish the limits of validity of the equivalent linearization approach.

INTRODUCTION

Current efforts to extend the performance and flight envelope of high-speed aerospace vehicles have resulted in structures which may respond to the imposed loads in a geometrically nonlinear (large deflection) random fashion. This type of behavior can significantly degrade the structural fatigue life. Linear prediction techniques currently used in the design process are grossly conservative and provide little understanding of the nonlinear behavior. Without practical design tools capable of capturing the important dynamics, further improvements in vehicle performance and system design will be hampered.

Methods currently used to predict geometrically nonlinear random response include perturbation, Fokker-Plank-Kolmogorov (F-P-K), numerical simulation and stochastic linearization techniques. All have various limitations. Perturbation techniques are limited to weak geometric nonlinearities. The F-P-K approach [1, 2] yields exact solutions, but can only be applied to simple mechanical systems. Numerical simulation techniques using numerical integration provide time histories of the response from which statistics of the random response may be calculated. This, however, comes at a high computational expense due to the long time records or high number of ensemble averages required to get quality random response statistics. Statistical linearization methods (e.g. equivalent linearization (EL), see [2-6]) have seen the most broad application because of their ability to accurately capture the response statistics over a wide range of response levels while maintaining relatively light computational burden. Implementations of

[†] Aerospace Engineer

[‡] Former NRC Postdoctoral Research Associate

statistical linearization methods have been primarily limited to special purpose “in-house” computer codes. The first known implementation in a general-purpose code was developed in [7] using MSC/NASTRAN. In this study, an alternative implementation of EL based on the methods developed in [8] and [9] will be used. This implementation was previously validated using the F-P-K method for a few special cases including a Duffing oscillator and beam structure under a convenient, but non-physical loading condition. In the present study, results from the EL analysis will be compared with those from a finite element based numerical simulation analysis for the case of a clamped-clamped beam under random inertial loading. By studying a wide range of load levels, the range of applicability is established.

EQUIVALENT LINEARIZATION APPROACH

The equations of motion of a multiple degree-of-freedom, viscously damped geometrically nonlinear system can be written in the form:

$$M\ddot{X}(t) + C\dot{X}(t) + KX(t) + \Gamma(X(t)) = F(t) \quad (1)$$

where M , C , K are the mass, damping, and stiffness matrices, X is the displacement response vector and F is the force excitation vector, respectively. The nonlinear stiffness term $\Gamma(X)$ is a vector function which generally includes 2nd and 3rd order terms in X . An approximate solution to (1) can be achieved by formation of an equivalent linear system:

$$M\ddot{X}(t) + C\dot{X}(t) + (K + K_e)X(t) = F(t) \quad (2)$$

where K_e is the equivalent linear stiffness matrix.

The traditional (force error minimization) method of EL seeks to minimize the difference between the nonlinear force and the product of the equivalent linear stiffness and displacement response vector. Since the error is a random function of time, the required condition is that the expectation of the mean square error be a minimum, i.e.:

$$error = E[(\Gamma(X) - K_e X)^T (\Gamma(X) - K_e X)] \rightarrow \min \quad (3)$$

where $E[...]$ represents the expectation operator. Equation (3) will be satisfied if

$$\frac{\partial(error)}{\partial K_{eij}} = 0 \quad i, j = 1, 2, \dots, N$$

In this study, consideration is limited to the case of Gaussian, zero-mean excitation and response to simplify the solution. With these assumptions and omitting intermediate derivations, the final form for the equivalent linear stiffness matrix becomes (see for example [3] and [4]):

$$K_e = E \left[\frac{\partial \Gamma}{\partial X} \right] \quad (4)$$

An alternative approach based on potential (strain) energy error minimization was proposed in [5] and [6], where mostly single degree-of-freedom systems were considered. A generalization for multiple degree-of-freedom systems is developed in [8] and [9]. For the sake of brevity, the present paper will present the formulation and results from the force error minimization only.

Applying the modal coordinate transformation

$$X = \Phi q$$

to equation (2) yields a set of coupled modal equations with reduced degrees of freedom, where Φ is generally a subset ($L \leq N$) of the linear eigenvectors, and q are the modal coordinates. This coupled set is expressed as:

$$[I]\ddot{q} + [2\zeta_r \omega_r] \dot{q} + [\omega_r^2] + [k_e] q = f \quad (5)$$

where ω_r are the undamped natural frequencies, $[I]$ is the unit matrix, $[2\zeta_r \omega_r]$ is the diagonal modal damping matrix, $[\omega_r^2]$ is the diagonal modal stiffness matrix, and $[k_e]$ is the fully populated equivalent stiffness matrix given by:

$$[k_e] = \left[E \left[\frac{\partial \gamma}{\partial q} \right] \right] \quad (6)$$

The nonlinear terms may be represented in the following form:

$$\gamma_r(q_1, q_2, \dots, q_L) = \sum_{j,k=j}^L a_{jk}^r q_j q_k + \sum_{j,k=j,l=k}^L b_{jkl}^r q_j q_k q_l \quad (7)$$

where a_{jk}^r and b_{jkl}^r are nonlinear stiffness coefficients with $j = 1, 2, \dots, L$, $k = j, j+1, \dots, L$, and $l = k, k+1, \dots, L$. This form of the nonlinear terms facilitates the solution of equations (5) when the forces and displacements are random functions in time.

Iterative Solution

Because the equivalent stiffness matrix k_e is a function of the unknown modal displacements, the solution takes an iterative form. The time variation of the modal displacements and forces may be expressed as:

$$q_r(t) = \sum_n \hat{q}_r e^{i\omega_n t} \quad f_r(t) = \sum_n \hat{f}_r e^{i\omega_n t} \quad (8)$$

where (^) indicates the dependency on ω_n . Applying (8) to (5) and writing in iterative form gives:

$$\hat{q}^m = [H^{m-1}] \hat{f} \quad (9)$$

where m is the iteration number and

$$[H^{m-1}] = [-\omega_n^2 [I] + i\omega_n [2\zeta_r \omega_r] + [\omega_r^2] + [\alpha k_e^{m-1} + \beta k_e^{m-2}]]^{-1} \quad (10)$$

The introduction of the weightings α and β are to aid in the convergence of the solution, with the condition that $\alpha + \beta = 1$.

For stochastic excitation, (9) is rewritten as:

$$[S_{qq}^m] = [H^{m-1}] [S_{ff}] [\bar{H}^{m-1}]^T \quad (11)$$

and

$$E[q_r q_s]^m = \sum_n S_{\hat{q}_r \hat{q}_s}^m \Delta \omega_n$$

The diagonal elements of $[S_{qq}^m]$ are the variances of the modal displacements. For the first iteration, $[k_e]$ is zero yielding the covariance matrix $E[q_r q_s]$ of the linear system. For subsequent iterations ($m > 1$), $[k_e^m]$ is determined from (6) as:

$$[k_e^m] = \left[E \left[\frac{\partial \gamma}{\partial q} \right] \right]^m = \begin{bmatrix} E \left[\frac{\partial \gamma_1}{\partial q_1} \right] & \cdots & E \left[\frac{\partial \gamma_1}{\partial q_L} \right] \\ \vdots & \ddots & \vdots \\ E \left[\frac{\partial \gamma_L}{\partial q_1} \right] & \cdots & E \left[\frac{\partial \gamma_L}{\partial q_L} \right] \end{bmatrix}^m \quad (12)$$

where (from (7)),

$$\left[E \left[\frac{\partial \gamma}{\partial q} \right] \right]^m = \begin{bmatrix} \sum_j^L a_{j1}^1 E[q_j] + \sum_{j,k=j}^L b_{jk1}^1 E[q_j q_k] & \cdots & \sum_j^L a_{jL}^1 E[q_j] + \sum_{j,k=j}^L b_{jkL}^1 E[q_j q_k] \\ \vdots & \ddots & \vdots \\ \sum_j^L a_{j1}^L E[q_j] + \sum_{j,k=j}^L b_{jk1}^L E[q_j q_k] & \cdots & \sum_j^L a_{jL}^L E[q_j] + \sum_{j,k=j}^L b_{jkL}^L E[q_j q_k] \end{bmatrix}^{m-1} \quad (13)$$

Recall a zero-mean response is assumed, i.e. $E[q] = 0$, which reduces (13) to:

$$\left[E \left[\frac{\partial \gamma}{\partial q} \right] \right]^m = \begin{bmatrix} \sum_{j,k=j}^L b_{jk1}^1 E[q_j q_k] & \cdots & \sum_{j,k=j}^L b_{jkL}^1 E[q_j q_k] \\ \vdots & \ddots & \vdots \\ \sum_{j,k=j}^L b_{jk1}^L E[q_j q_k] & \cdots & \sum_{j,k=j}^L b_{jkL}^L E[q_j q_k] \end{bmatrix}^{m-1} \quad (14)$$

The iterations continue until convergence of the equivalent stiffness matrix such that

$$\| [k_e^m] - [k_e^{m-1}] \| < \varepsilon$$

The value of ε typically used is 0.1%. Following convergence, the $N \times N$ covariance matrix of the displacements in physical coordinates is recovered from

$$E[X_i X_j] = \Phi E[q_r q_s] \Phi^T \quad (15)$$

and root-mean-square values are the square roots of the diagonal terms in (15). Further post-processing to obtain power spectral densities of displacements, stresses, strains, etc., may be performed by substituting the converged equivalent stiffness matrix into (5) and solving in the usual linear fashion.

Implementation

The EL procedure as outlined above was recently implemented within the context of MSC/NASTRAN using the DMAP programming language [10]. The implementation entails first performing a normal modes analysis (solution 103) to obtain the modal matrices, from which a subset of L modes are chosen. Since the form of the nonlinear stiffness terms are not explicitly known, the nonlinear stiffness coefficients a_{jk}^r and b_{jkl}^r must be determined numerically. To accomplish this, a series of inverse problems are performed by prescribing displacement fields as linear combinations of modes to the linear static (solution 101) and nonlinear static (solution 106) solutions. The nonlinear stiffness coefficients are then determined from the resulting linear and nonlinear nodal forces. The process by which this is done is covered in detail in [8] and [9]. The iterative solution is performed within a standalone DMAP alter, which has as its output the root-mean-square displacements in physical coordinates, the cross covariance in modal coordinates, and the sum of the linear and equivalent linear modal stiffness matrices. The latter may be substituted for the linear modal stiffness in the modal frequency response analysis (solution 111) for post-processing.

NUMERICAL SIMULATION APPROACH

A numerical simulation analysis was performed to generate time history results from which response statistics could be calculated. The particular method used was finite element based with the integration performed in physical coordinates. Two different integration methods were used depending on the response level. For lower level responses, an implicit integration method was taken which allowed for larger time steps compared with the explicit method. Because the implicit scheme is unconditionally stable, a convergence study on the time step was undertaken at each response level to ensure adequacy of the time step. This was done by halving the Δt used until the time history response over the calculation period was unchanged. As the response level became higher at the higher excitation levels, the Δt required to obtain a converged solution became smaller. When the Δt required was on the order of the time step required for the explicit method, it became more efficient to perform the explicit integration. Both methods produced identical results, so the particular choice of implicit versus explicit was dictated solely by the time required to run each analysis. In both the implicit and explicit methods, the nonlinear deformation was handled using a corotational scheme [11]. The program NONSTAD [12] was used to generate the numerical simulation results.

Loading Time History

The time history of the load was generated by summing equal amplitude sine waves with random phase within a specified bandwidth using a discrete inverse Fourier transform. This generated a pseudo-random time history with a specified amplitude and period T . The period was specified by $2^n \Delta t$. In this study, $\Delta t = 50 \mu s$ and $n = 16$, giving a period of $1.6384 s$ in duration. The selected Δt corresponded with that needed for the implicit integration scheme used for the lower loading levels. The explicit integration scheme used for the higher load levels interpolated the signal between points such that the specified loading at each Δt interval was maintained. A radix-2 number of time history samples was chosen to facilitate use of radix-2 FFT algorithms employed for the subsequent analysis. An ensemble of time histories was generated by specifying different seeds to the random number generator.

A typical time history corresponding to an inertial load of $0.05g$ RMS is shown in Figure 1. The corresponding probability density function is also shown with the Gaussian distribution. The power spectral density for 10 ensemble averages gives a spectrum level of $1.67 \times 10^{-6} g^2/Hz$ over a $1500 Hz$ bandwidth as shown. A sharp roll-off of the input spectrum practically eliminates excitation of the structure outside the frequency range of interest.

Transient Response Processing

The structure is assumed to be at rest at the beginning of each loading. An initial transient in the structural response is therefore induced before the response becomes fully developed. This transient must be eliminated to ensure the proper response statistics are recovered.

The approach taken to eliminate the transient is shown graphically in Figure 2. Because the loading is pseudo-random, it is possible to apply multiple periods of the load and generate the same statistics for periods of length T beginning at any point in time. For example, the statistics of the load are the same for the period $0 - T$ as they are for the period $T/4 - 5T/4$. In a like manner, for the linear condition, the response statistics are the same for any period T following the initial transient. Therefore, by computing the desired statistic for a moving window of period T , it is possible to identify a point in time t_o after which the response statistics do not change significantly. In the present study, the root-mean-square response was monitored and a time of $t_o = 0.5s$ was found suitable. For each loading history, a total response of $T + 0.5s = 2.1384s$ was calculated and the first $0.5s$ was discarded. Note that a similar argument for the nonlinear condition does not hold because the nonlinear response is not periodic over T . Nevertheless, the above approach was employed with satisfactory results.

Response Statistics

Response statistics were generated from an ensemble of $N=10$ time histories at each load level. Estimates of the displacement root-mean-square served as the basis for comparison with the EL method, which essentially had the RMS as its basic unknown. Additionally, confidence intervals for the mean value of the RMS estimate were generated to quantify the degree of uncertainty in the estimate [13] using:

$$\left[\bar{x} - \frac{St_{n;\alpha/n}}{\sqrt{N}} \leq \mu_x < \bar{x} + \frac{St_{n;\alpha/n}}{\sqrt{N}} \right], \quad n = N - 1$$

where \bar{x} and s^2 are the sample mean and variance of the RMS estimates from N ensembles, and t_n is the Student t distribution with n degrees of freedom, evaluated at $\alpha / 2$. For the 90% confidence intervals calculated, $\alpha = 0.1$.

Estimates of the displacement mean, skewness, and kurtosis were also computed to help ascertain the degree to which the assumptions made in the development of the equivalent linearization method were followed. Power spectral density and probability density functions of the displacement were computed for similar purposes.

RESULTS

Validation studies were conducted using an 18-in. x 1-in. x 0.09in. ($l \times w \times h$) clamped-clamped aluminum beam with material properties:

$$E = 10.6 \times 10^6 \text{ psi}, \quad G = 4.0 \times 10^6 \text{ psi}, \quad \rho = 2.588 \times 10^{-4} \frac{\text{lb}_f \cdot \text{s}^2}{\text{in}^4}$$

The beam was subjected to an inertial loading over a computational bandwidth of 1500 Hz, as shown in Figure 1. This bandwidth was in excess of the desired bandwidth of 1000 Hz to allow for the contribution of the higher order modes in the EL solution. This is especially important for capturing the anti-resonant behavior. The numerical simulation analysis utilized the same loading for consistency, although the effect of the higher order modes are automatically realized since the computations are performed in physical coordinates. Since the loading was uniformly distributed, only symmetric modes were included in the analysis. In general, any combination of symmetric and non-symmetric modes may be included.

The NASTRAN model used in the EL analysis was comprised of thirty-six 1/2-in. long CBEAM elements. The EL analysis used a four-mode solution comprised of the first four symmetric bending modes. Damping was chosen to be consistent with the mass-proportional damping of the numerical simulation analysis and at a level sufficiently high so that a good comparison could be made at the peaks of the PSD. This dictated a critical damping of 2.0%, 0.37%, 0.15%, and 0.081% for the first four symmetric modes. The finite element model used in the numerical simulation analysis was also comprised of thirty-six 1/2-in. long beam elements. Both EL and simulation finite

element models were checked for convergence by running additional analyses with models consisting of 1/4-in. elements.

Analysis was performed at load levels of 0.8, 3.2, 12.8, 51.2, and 204.8 g RMS, giving a dynamic range of 48 dB. Figure 3 shows the normalized RMS out-of-plane (w) deflection at the beam center as a function of load level. The numerical simulation results are shown with 90% confidence intervals of the RMS estimate. At the lowest load level of 0.8 g RMS, the response is linear as can be seen by the comparison with results from a strictly linear analysis (NASTRAN solution 111). A small, but noticeable, difference between the linear and nonlinear response is noted at the 3.2g RMS load level. The degree of nonlinearity increases with load level, as expected. At the highest load level, the nonlinear response calculations predict a RMS center deflection of 2.5 times the thickness compared with the nearly 11 times the thickness from the linear analysis.

In order to gain greater insight into the nonlinear dynamics, plots of the time history, PSD, and PDF are shown for three load levels, 0.8, 51.2 and 204.8g RMS, in Figure 4 through Figure 6, respectively. Data in the time history and PDF plots correspond solely to numerical simulation results. Data in the PSD plots correspond to numerical simulation and EL results, where the EL results were generated by running a linear analysis (NASTRAN solution 111) using the equivalent linear stiffness generated by the EL process described above. Also shown in the figures are plots of the normalized RMS deflection shape for both numerical simulation and EL analyses.

Results for the 0.8g RMS excitation level are shown in Figure 4. This excitation level was shown (see Figure 3) to produce a linear response. As expected, the PDF mimics the normally distributed PDF of the input shown in Figure 1. The averaged PSD and normalized deflected shape show excellent agreement between the EL and numerical simulation results. This agreement helps to establish the confidence in making comparisons between these two fundamentally different analyses.

Figure 5 shows a nonlinear response associated with the 51.2g RMS excitation level. The time history of the center displacement has a visibly higher peak probability and the PDF exhibits a flattening at the peak. The PSD from both the numerical simulation and EL analyses both show the shifting of peaks to higher frequencies compared with the linear solution. This shifting is associated with a hardening spring type of nonlinearity. Note that the frequencies associated with the peaks of the EL solution are the natural frequencies of the equivalent linear system. The numerical simulation results correctly show the peak broadening effect, which the EL analysis is unable to capture. Also distinguishable in the numerical simulation results are contributions of harmonics. The effect of nonlinearity is somewhat over predicted in the EL result, as seen in the normalized deflection shape.

The highest degree of nonlinearity is shown in Figure 6, corresponding to the 204.8g RMS load. The time history is further peak oriented and the PDF is nearly flat. The peak broadening in the PSD of the numerical simulation results is severe, and nearly flattens the spectrum above 350 Hz. Of particular interest is flattening of the normalized deflection shape, which both the EL and numerical simulation results reflect. This is likely to have a significant effect on the strain distribution. It is unclear why the results at the 204.8g RMS load level compare more favorably than those at the 51.2g RMS level. This behavior warrants further investigation.

Moments of the center displacement were calculated from the numerical simulation results for all load levels. They are provided in Table 1 with the RMS center displacement from the EL analysis. The EL and numerical simulation results agree well, thus validating the EL analysis over a substantial load range. The validity of assumptions made in the development of the EL method are ascertained by observing the mean, skewness and kurtosis. The mean value is effectively zero for all load levels, indicating the assumption of zero mean response has not been violated. Although the PDF is more or less skew-symmetric, the shape is flattened at the higher load levels as indicated by a decreasing kurtosis from the linear value of 3. The decreasing kurtosis values indicate a violation of the Gaussian response assumption. However, even with this non-Gaussian response distribution, the EL analysis gives a good prediction of the RMS response.

Table 1: Moments of the center displacement.

Load (g) _{RMS}	Mean (in.)	EL RMS (in.)	Numerical Simulation RMS (90% Confidence Interval) (in.)	Skewness	Kurtosis
0.8	-6.54×10^{-8}	0.0038	$0.00379 \leq \text{RMS} < 0.00381$	0.0197	3.05
3.2	-5.26×10^{-6}	0.0147	$0.01438 \leq \text{RMS} < 0.01532$	0.0190	2.82
12.8	-1.62×10^{-5}	0.0458	$0.04680 \leq \text{RMS} < 0.05350$	-0.0017	2.47
51.2	-4.93×10^{-6}	0.1078	$0.11268 \leq \text{RMS} < 0.12325$	-0.0002	2.25
204.8	3.78×10^{-4}	0.2285	$0.21654 \leq \text{RMS} < 0.23216$	-0.0058	2.29

DISCUSSION

The RMS random response predictions from the EL implementation have been validated through a wide range of load levels. Comparisons with numerical simulation results are good, even when the assumption of Gaussian response has been violated.

Differences that do exist warrant some discussion. It is seen that the EL approach slightly over-predicts the degree of nonlinearity compared to the numerical simulation results. This does not appear to be due to a violation of the assumption of a Gaussian response because the over-prediction does not correlate with increasing kurtosis of response. The likely reason for the difference is in the error minimization approach used. Results previously

computed using the alternative strain-energy error minimization technique, not included here, indicated better comparison with the exact F-P-K solution than the conventional force-based error minimization undertaken here [9]. The improved comparison of strain-energy error minimization and simulation results was also seen in a different EL implementation for the problem of a beam on an elastic foundation [6]. The strain-energy analysis is beyond the scope of this paper and is left as an area for further investigation.

Some implications on the use of the EL technique as a basis for fatigue life calculations are worth mentioning. First, assuming that stresses or strains from the EL technique will compare equally well with the fully nonlinear results, a simple fatigue-life calculation based on RMS levels will be much less conservative than calculations based on linear analyses. This offers the potential for substantial weight savings for structures designed using nonlinear methods. Secondly, it appears that a nonlinear analysis, EL or otherwise, is required to accurately calculate the RMS deflected shape. Use of a linear RMS deflected shape scaled to the nonlinear level would inaccurately reflect the spatial distribution. Simple fatigue-life calculations based on the RMS stress or strain could be significantly affected as these quantities depend on the spatial distribution of the deformation. Lastly, use of the EL derived PSD response in a more sophisticated fatigue-life calculation requires careful investigation. Recall that peaks in the equivalent linear PSD may occur at different frequencies than the fully nonlinear PSD, as shown in Figure 5 and Figure 6. Methods such as spectral fatigue analysis [14], which take moments of the PSD, may incorrectly account for the contribution a particular frequency component in the cycle counting scheme. It is not known, for example, if the narrowly shaped, higher fundamental frequencies of the equivalent linear PSD result in conservative or non-conservative estimates of fatigue life relative to predictions made using the fully nonlinear PSD with more broadly shaped, lower fundamental frequencies. An assessment of this effect is left as an area for further study.

The question of computational efficiency has not been addressed in this paper because the differing analyses were performed on different computer platforms. What can be stated is that the computational burden for the EL approach will increase only slightly with an increase in the size of the physical model for the same number of modes used in the solution. This increase is associated with the solution of a larger linear eigenvalue problem. The expense of the numerical simulation solution, however, will increase dramatically with an increase in physical system size.

ACKNOWLEDGEMENTS

The authors wish to thank Professor James F. Doyle of Purdue University for providing the finite element code NONSTAD used for the numerical simulation analysis and for his advise on its use. The authors also thank

Travis Turner and Jay Robinson of NASA Langley Research Center for helpful discussions and comments.

REFERENCES

1. Bolotin, V.V., Statistical methods in structural mechanics. 1969: Holden-Day, Inc.
2. Lin, Y.K., Probabilistic theory of structural dynamics. 1976, Malabar, FL: R.E. Krieger.
3. Roberts, J.B. and Spanos, P.D., Random vibration and statistical linearization. 1990, New York, NY: John Wiley & Sons.
4. Atalik, T.S. and Utku, S., Stochastic linearization of multi-degree-of-freedom nonlinear systems, *Earthquake engineering and structural dynamics*, 1976, **4**, pp. 411-420.
5. Elishakoff, I. and Zhang, R. Comparison of new energy-based versions of the stochastic linearization technique. In *IUTAM Symposium*, Turin, Springer-Verlag, 1992, pp. 201-211.
6. Fang, J. and Elishakoff, I., Nonlinear response of a beam under stationary excitation by improved stochastic linearization method, *Applied Mathematical Modelling*, 1995, **19**, pp. 106-111.
7. Robinson, J.H., Chiang, C.K., and Rizzi, S.A., Nonlinear Random Response Prediction Using MSC/NASTRAN, NASA TM 109029, October 1993.
8. Muravyov, A.A., Turner, T.L., Robinson, J.H., Rizzi, S.A. A new stochastic linearization implementation for prediction of geometrically nonlinear vibrations. In *40th AIAA/ASCE/AHS/ASC Structures, Structural Dynamics and Materials Conference*, St. Louis, MO, AIAA, 1999, pp. 1489-1497.
9. Muravyov, A.A. Determination of nonlinear stiffness coefficients for finite element models with application to the random vibration problem. In *MSC Worldwide Aerospace Conference Proceedings*, Long Beach, MacNeal-Schwendler Corp., 1999, pp. 1-14.
10. Bella, D. and Reymond, M., eds. *MSC/NASTRAN DMAP Module Dictionary*. Version 68 ed. . 1994, MacNeal-Schwendler Corporation: Los Angeles, CA.
11. Crisfield, M.A., Nonlinear finite element analysis of solids and structures. Vol. 2. 1997: Wiley.
12. Doyle, J.F., Lecture Notes: AAE 546 - Static and dynamic analysis of thin-walled structures. 1999: Purdue University.
13. Bendat, J.S. and Piersol, A.G., Random data: Analysis and measurement procedures. 1971: Wiley-Interscience.
14. Bishop, N.W.M. and Sherratt, F., A theoretical solution for the estimation of rainflow ranges from power spectral density data, *Fat. Fract. Engng. Mater. Struct.*, 1990, **13**, pp. 311-326.

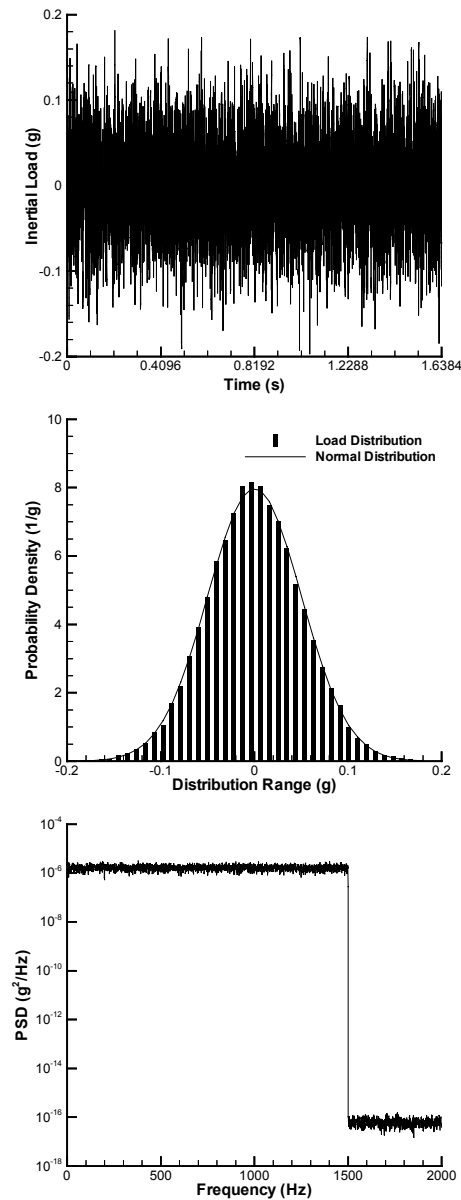


Figure 1: Typical loading time history, probability density, and power spectral density.

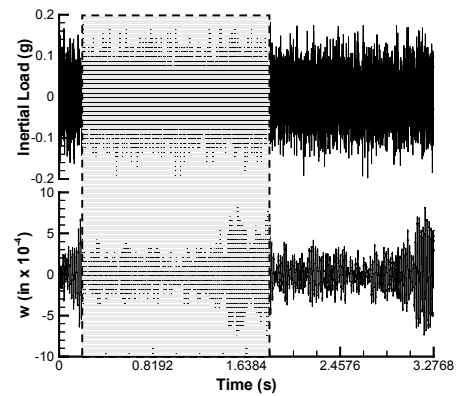


Figure 2: Transient response processing.

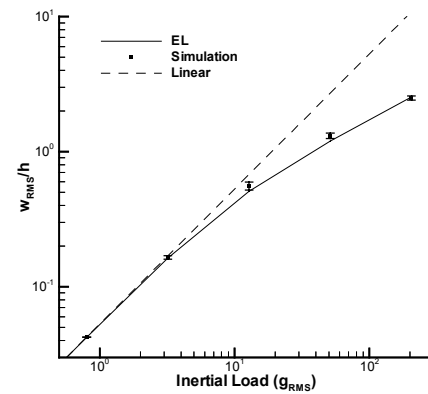


Figure 3: Normalized RMS center deflection as a function of inertial load

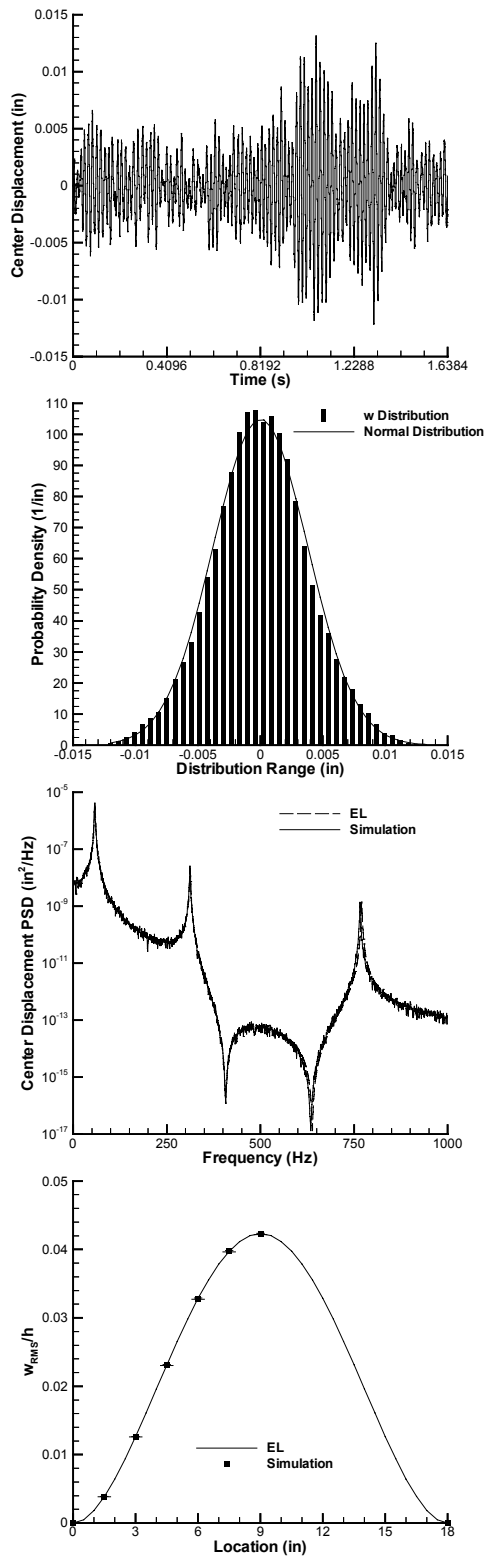


Figure 4: Center deflection response and normalized deflection shape at 0.8g RMS inertial load.

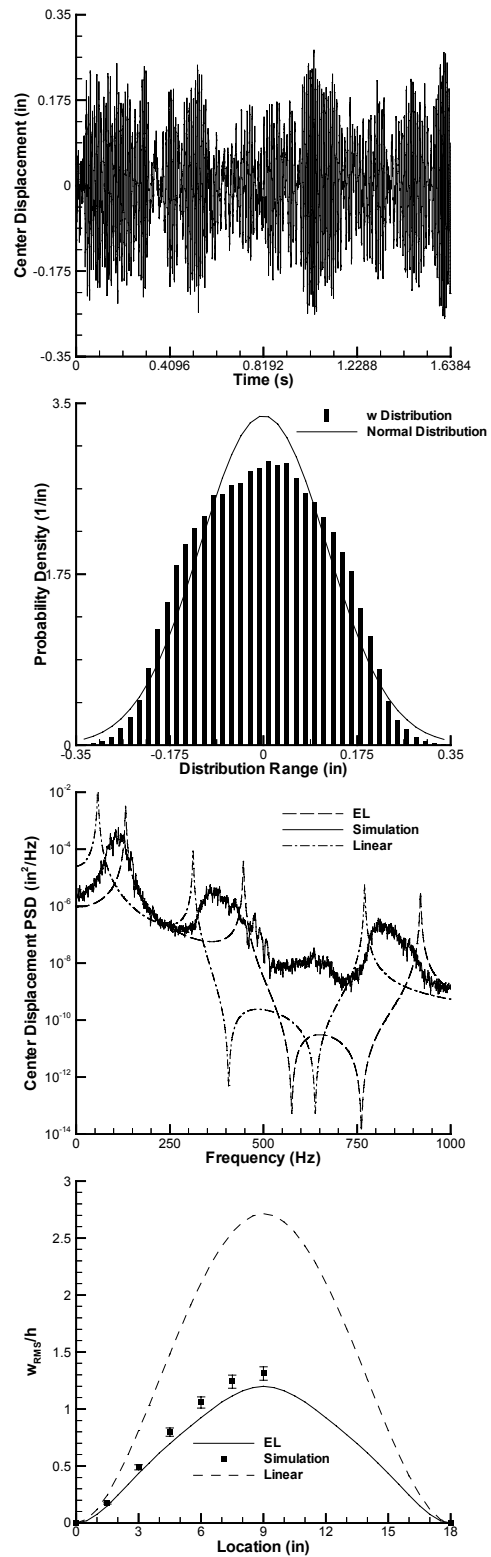


Figure 5: Center deflection response and normalized deflection shape at 51.2g RMS inertial load.

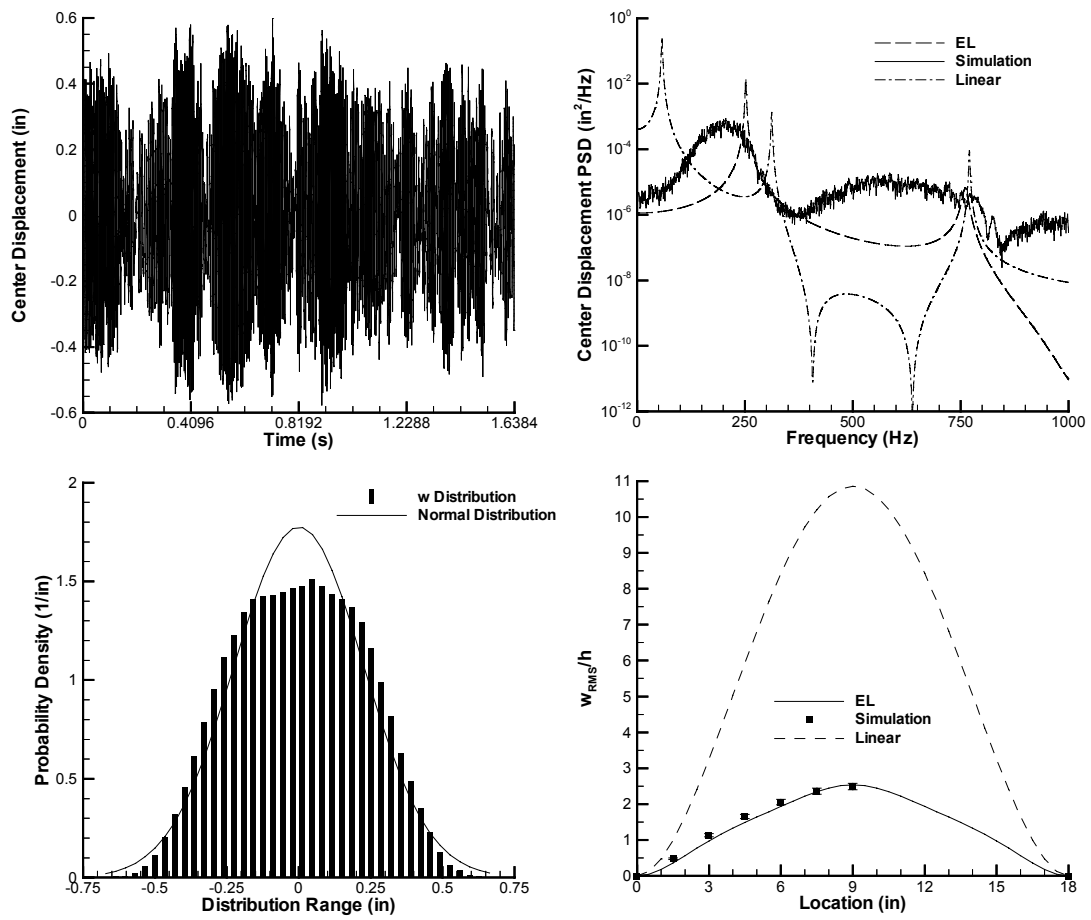


Figure 6: Time history, PSD, and PDF of center deflection response and normalized deflection shape at 204.8g RMS inertial load.